

TeV Gamma-Ray Observations of the Galactic Center

K. Kosack,¹ H. M. Badran,² I. H. Bond,³ P. J. Boyle,⁴ S. M. Bradbury,³ J. H. Buckley,¹ D. A. Carter-Lewis,⁶ M. Catanese,⁵ O. Celik,⁷ V. Connaughton,²¹ W. Cui,⁸ M. Daniel,⁶ M. D'Vali,³ I. de la Calle Perez,³ C. Duke,⁹ A. Falcone,⁸ D. J. Fegan,¹⁰ S. J. Fegan,⁵ J. P. Finley,⁸ L. F. Fortson,^{19,20} J. A. Gaidos,⁸ S. Gammell,¹⁰ K. Gibbs,⁵ G. H. Gillanders,¹¹ J. Grube,³ J. Hall,¹² T. A. Hall,¹³ D. Hanna,¹⁴ A. M. Hillas,³ J. Holder,³ D. Horan,⁵ A. Jarvis,⁷ M. Jordan,¹ G. E. Kenny,¹¹ M. Kertzman,¹⁵ D. Kieda,¹² J. Kildea,¹⁴ J. Knapp,³ H. Krawczynski,¹ F. Krennrich,⁶ M. J. Lang,¹¹ S. Le Bohec,⁶ R. W. Lessard,⁸ E. Linton,⁴ J. Lloyd-Evans,³ A. Milovanovic,³ J. McEnery,¹⁷ P. Moriarty,¹⁶ D. Muller,⁴ T. Nagai,¹² S. Nolan,⁸ R. A. Ong,⁷ R. Pallassini,³ D. Petry,¹⁷ B. Power-Mooney,¹⁰ J. Quinn,¹⁰ M. Quinn,¹⁶ K. Ragan,¹⁴ P. Rebillot,¹ P. T. Reynolds,¹⁸ H. J. Rose,³ M. Schroedter,⁵ G. H. Sembroski,⁸ S. P. Swordy,⁴ A. Syson,³ V. V. Vassiliev,⁷ S. P. Wakely,⁴ G. Walker,¹² T. C. Weekes,⁵ J. Zweerink,⁷

kosack@hbar.wustl.edu buckley@wuphys.wustl.edu

¹Department of Physics, Washington University, St. Louis, MO 63130, USA

²Physics Department, Tanta University, Tanta, Egypt

³Department of Physics, University of Leeds, Leeds, LS2 9JT, Yorkshire, England, UK

⁴Enrico Fermi Institute, University of Chicago, Chicago, IL 60637, USA

⁵Fred Lawrence Whipple Observatory, Harvard-Smithsonian CfA, P.O. Box 97, Amado, AZ 85645-0097

⁶Department of Physics and Astronomy, Iowa State University, Ames, IA 50011-3160, USA

⁷Department of Physics, University of California, Los Angeles, CA 90095-1562, USA

⁸Department of Physics, Purdue University, West Lafayette, IN 47907, USA

⁹Department of Physics, Grinnell College, Grinnell, IA 50112-1690, USA

¹⁰Experimental Physics Department, National University of Ireland, Belfield, Dublin 4, Ireland

¹¹Department of Physics, National University of Ireland, Galway, Ireland

¹²High Energy Astrophysics Institute, University of Utah, Salt Lake City, UT 84112, USA

¹³Department of Physics and Astronomy, University of Arkansas at Little Rock, Little Rock, AR 72204-1099, USA

¹⁴Physics Department, McGill University, Montréal, QCH3A 2T8, Canada

¹⁵Department of Physics and Astronomy, DePauw University, Greencastle, IN 46135-0037, USA

¹⁶School of Science, Galway-Mayo Institute of Technology, Galway, Ireland

¹⁷University of Maryland, Baltimore County and NASA/GSFC, USA

¹⁸Department of Applied Physics and Instrumentation, Cork Institute of Technology, Cork, Ireland

¹⁹Department of Astronomy and Astrophysics, University of Chicago, Chicago, IL, USA

²⁰Astronomy Department, Adler Planetarium and Astronomy Museum, Chicago, IL, USA.

²¹Gamma-Ray Astrophysics Group National Space Science and Technology Center Huntsville, Alabama

ABSTRACT

We report a possible detection of TeV gamma-rays from the Galactic Center by the Whipple 10m gamma-ray telescope. Twenty-six hours of data were taken over an extended period from 1995 through 2003 resulting in a total significance of 3.7 standard deviations. The measured excess corresponds to an integral flux of $1.6 \times 10^{-8} \pm 0.5 \times 10^{-8}(\text{stat}) \pm 0.3 \times 10^{-8}(\text{sys})$ photons $\text{m}^{-2} \text{s}^{-1}$ above an energy of 2.8 TeV, roughly 40% of the flux from the Crab Nebula at this energy. The 95% confidence region has an angular extent of about 15 arcmin and includes the position of Sgr A*. The detection is consistent with a point source and shows no evidence for variability.

1. Introduction

The central region of our galaxy is now thought to contain a super-massive black-hole of $2.6 \times 10^6 M_\odot$ (Ghez et al. 2002; Schödel et al. 2002) coincident with the unresolved radio source Sgr A* (Balick & Brown 1974). Chandra observations reveal X-ray emission from an unresolved point source as well as an extended structure (~ 1.5 arcsec), both of which appear to be physically associated with Sgr A* (e.g., Baganoff et al. (2003)). The recent discovery of hour-scale X-ray (Baganoff et al. 2001) and rapid IR flaring (Ghez et al. 2004) point to an active nucleus, albeit with very low bolometric luminosity compared with the luminosity inferred from the Bondi accretion rate or with that which is typical of more powerful AGNs. More recently, *INTEGRAL* (*the International Gamma-Ray Astrophysics Laboratory*) has detected time-variable 20-100 keV emission from within $0.9'$ of Sgr A* (Bélanger et al. 2004). Polarization measurements show the signature of synchrotron radiation in a Keplerian accretion disk (Liu & Melia 2002). Taken together, these multi-wavelength data are not easily described by a one-component model, and the current theoretical framework combines thermal emission from a radiatively inefficient Keplerian accretion flow with synchrotron inverse-Compton emission produced either by electrons accelerated in the disk or further out in a hypothetical jet-like outflow (e.g. Liu & Melia (2002); Yuan, Markoff, & Falcke (2002); Yuan, Quataert, & Narayan (2003)). From the present measurements, the maximum energy of the non-thermal electron distribution in the jet models is ambiguous and theories alternately explain the high-energy emission as inverse-Compton or the high-energy extension of the synchrotron spectrum; gamma-ray measurements may eventually break this degeneracy.

The EGRET experiment detected a strong unidentified source of GeV gamma-rays marginally consistent with the position of the Galactic Center (Hartman et al. 1999). Both the Whipple and Cangaroo groups have presented preliminary evidence for TeV emission at the position of Sgr A* as well (Buckley et. al. 1997; Tsuchiya et al. 2003; Kosack et. al. 2003). Hooper & Dingus (2002) re-analyzed the higher energy gamma-ray data from EGRET and found that the most likely position of the EGRET source may be offset from Sgr A*. However, systematic uncertainties in the gamma-ray background models and limited angular resolution make the analysis of the source in

the Galactic Center region difficult. Observations of the Galactic Center are complicated since Sgr A* is surrounded by a dense cluster of stars and stellar remnants (including low-mass X-ray binaries and black hole candidates), molecular clouds, and a large structure that may be the remnant of a powerful supernova remnant, Sgr A East (Fatuzzo & Melia 2003). Source confusion is particularly difficult for high-energy gamma-ray observations given the limited angular resolution of present experiments.

High energy gamma-ray observations of the Galactic Center are also the subject of particular theoretical interest given the possibility of detecting halo dark matter in our galaxy (e.g. Bergström, Ullio, & Buckley (1998)). Sgr A*, at the dynamical center of our galaxy, may well be surrounded by a cusp or spike in the dark matter halo distribution (e.g. Dubinski & Carlberg (1991); Navarro, Frenk, & White (1996); Gondolo & Silk (1999); Merritt (2003)). Annihilation of these hypothetical weakly interacting massive particles could also contribute to the luminosity in the vicinity of Sgr A* in the radio through gamma-ray waveband. Annihilation of dark matter would be enhanced by a factor proportional to the density squared, and might result in an observable gamma-ray line (from direct annihilation to gamma rays) as well as continuum emission (from secondary products of annihilation to quarks and fermions) (Silk & Bloemen 1987; Bergstrom 1989; Rudaz 1989; Giudice & Griest 1989; Stecker & Tylka 1989; Jungman & Kamionkowski 1995). The presence of a massive black hole could further steepen the density profile of the dark matter halo, producing very high radio and gamma-ray fluxes that exceed the observational upper bounds (Gondolo & Silk 1999). The details of the halo model on scales $< 100\text{pc}$ and the formation history of the central black hole are critical to predicting the gamma-ray flux, but are, unfortunately, still poorly understood.

Given the limited angular resolution of GeV and TeV instruments, a number of different sources could contribute to a signal near the Galactic Center. The key to distinguishing between all of the possible emission scenarios is to measure the position, angular extent, variability and spectrum of the gamma-ray signal. Here we present first results from an analysis of Whipple telescope data. In §2 we describe the observational method and data analysis procedure used to observe the Galactic Center at TeV energies. In §3 and §4, we discuss a possible weak detection and consider its impact on various gamma-ray production scenarios in §5.

Season(s)	F.O.V (°)	Pixels	Pixel Diameter(°)
1995-1996	3.1	109	0.26
1996-1997	3.1	151	0.26
1999-2003	2.4	379	0.12

Table 1: Camera specifications during seasons where Galactic Center data were taken.

2. Method

Imaging Atmospheric Čerenkov Telescopes (IACTs), like the Whipple Gamma-ray Observatory, detect high energy photons by imaging the flashes of Čerenkov light emitted by secondary particles in gamma-ray induced air showers. The Whipple Telescope’s 10m mirror focuses the faint UV/blue Čerenkov flashes into a camera consisting of 379 photomultiplier tube pixels (for the latest seasons—see Table 1 for previous seasons). Off-line software analysis characterizes each candidate shower image, separates signal (gamma-ray-like) from background (cosmic-ray-like) events, and determines the point of origin and energy of each gamma ray.

Whipple gamma-ray data are traditionally taken as a series of 28 minute exposures, each of which is followed by an off-source run which is offset 30 minutes in right ascension for background subtraction. In the case of Sgr A*, data were taken off-source before the on-source observations due to a bright star field in the region 30 minutes past the Galactic Center’s position. The analysis method used here (see §3) was modified to give sensitivity at large zenith angles and to provide a two-dimensional map of the TeV emission in a three-degree diameter field-of-view surrounding the Galactic Center.

3. Data Analysis

The Galactic Center ($\alpha = 17^h45^m40^s$, $\delta = -29^\circ00'28''$, J2000) transits at a very large zenith angle (61°) as seen from the Whipple Observatory (31.7° N latitude) which significantly alters the shower geometry and threshold energy. To properly account for the effects of LZA observations, special techniques that go beyond the standard Whipple analysis were required. Furthermore, the brightness of the galactic plane near the Galactic Center results in an increase in energy threshold and, if not compensated for, a systematic bias in the observed excess. Pedestal events, containing no image, are injected at random intervals throughout the run for calibration of Poisson fluctuations in the night sky background. Both on and off-source data are analyzed in the same manner, and Gaussian deviates are added to the pixel signals to bring the background noise up to the same level in both runs. After this procedure, only pixels with signals well above the noise level are included in further image processing. This Gaussian *padding* combined with a high software trigger threshold largely removes systematic biases arising from brightness differences, but increases the energy threshold.

Using the techniques based on the moment fitting procedure outlined in Reynolds et al. (1993), we parameterize the roughly elliptical gamma-ray images by calculating moments of the light distribution in the camera. Geometric selection criteria based on these parameters allow for the rejection of background (e.g. cosmic-ray induced showers). The first moments give the centroid of the image, the second moments give the WIDTH (minor axis) and LENGTH (major axis) and orientation angle of the image. The elongation of the ellipse is used to determine the point of origin of each shower image using the formula $\delta = \epsilon \left(1 - \frac{\text{WIDTH}}{\text{LENGTH}}\right)$, where δ is the displacement of the point of

origin from the image centroid and ϵ is the elongation factor (determined by simulations). Of the two possible points of origin for each image, the asymmetry (or skew) of the shower is used to select the correct one whenever possible. This procedure is similar to that described in Lessard et al. (2001).

To determine the pointing error in the telescope, we look at the pedestal variation for each tube. The presence of visible light from a star or other source of sky brightness in the field of view adds to the pedestal variance in the corresponding photomultiplier tube. Using this effect, we can generate a crude optical image of the sky by de-rotating the camera to a common orientation (since the field of view rotates with time for an altitude-azimuth telescope) and accumulating the pedestal variations of each pixel into a two-dimensional histogram. Using this technique, an optical *sky-brightness* map is generated for each observation. By comparing the bright spots in the Sgr A* image (or special runs where the telescope is pointed at a nearby *pointing-check* star) we can obtain an absolute measure of the pointing error. In addition, we cross-correlate each pair of maps to determine the relative pointing offset between them. We only keep runs that have the correct star field and have a relative pointing offset (compared with the other Sgr A* runs) which is less than the diameter of one pixel. This lessens the possibility of accidentally including an observation with large pointing errors or which was mislabeled. Using this method, we find residual pointing errors of $\pm 0.1^\circ$ and an absolute offset of 0.14° . These errors are attributed in part to the fact that observations have been made near the balance point of the telescope and near the horizontal position where flexure of the optical support structure is maximal.

Sgr A* transits at roughly 30° elevation as observed from the latitude of the Whipple Observatory. Large zenith angle (LZA) observations require several modifications to the standard analysis due to changes in shower geometry. In addition, we have data on Sgr A* that spans several epochs during which the Whipple camera was upgraded twice (see Table 1). In order to combine all of these data, we needed our gamma-ray selection criteria to scale properly with changes in zenith angle, the camera throughput factor (i.e. the ratio of photons hitting the mirror to digital counts in the digitized PMT signals), and the pixel size. In addition, for subsequent spectral analysis, we designed our gamma-ray selection procedure to scale with energy to minimize spectral biases.

To achieve this goal, we started with the standard Whipple Telescope data analysis procedure (Lessard et al. 2001) and developed a new set of gamma-ray selection criteria that scale with zenith angle and energy according to a semi-empirical form derived from simulations and optimization of LZA Crab Nebula data. Our criteria also incorporate the geometric effects of differing cameras, allowing us easily to combine all of the data present for the Galactic Center. The Crab Nebula was used for optimization and calibration because it is a bright, steady gamma-ray source with a known spectrum. In addition, an independent set of Crab Nebula observations taken at LZA were used to verify that the selection criteria were more efficient than the standard analysis procedure.

To correct for changes in the overall light sensitivity (throughput) of the camera between epochs, we look at muon events in data taken at each epoch. Muons, which show up as bright arcs

of Čerenkov light in the camera, are useful for throughput calibration because the light per unit arc-length from a muon event is nearly constant regardless of the impact parameter and angle of the trajectory. A measure of the throughput of the telescope can be found by making a histogram of the *signal/arc-length* distribution of a large set of muon events. To get an absolute calibration, this distribution for real observations was compared with a set of simulated muon events which were generated using the Grinnell/ISU (GrISU) simulation package to produce a large number of H and He showers that in turn produce muons as secondary particles. For instance, the relative throughput was found to have changed by a factor of 2.22 between 1995 and 2001. We scale the software trigger threshold and energy estimator by this factor so the trigger cuts are consistent across observations. This method also serves to calibrate the simulations used to determine the peak energy at LZA (see §4).

As one observes at increasing zenith angles, the distance to the core of the air-shower increases and thus the angular size of the shower and parallactic displacement of the image centroid are reduced. To derive the scaling laws, we first assume that the WIDTH and LENGTH of gamma-ray air shower images is approximately proportional to $\cos^\alpha \theta$, where θ is the zenith angle and α is a constant. Additionally, air-shower simulations show that LENGTH and WIDTH also scale as the logarithm of the energy, which is proportional to the SIZE (total camera signal) of the event.

Combining these results, and removing the effects of the finite pixel size of the camera (σ_{pix}) and the point spread function of the telescope (σ_{psf}), the measured LENGTH (L), WIDTH (W), and the distance to the image centroid (D) can be converted to scaled values L' , W' and D' by the following equations:

$$\Sigma \equiv \ln(\text{SIZE}) - 8.0$$

$$L' \simeq \left[\frac{L^2 - \sigma_{\text{pix}}^2 - \sigma_{\text{psf}}^2}{\cos^{1.5} \theta} \right]^{\frac{1}{2}} - 0.023\Sigma \quad (1)$$

$$W' \simeq \left[\frac{W^2 - \sigma_{\text{pix}}^2 - \sigma_{\text{psf}}^2}{\cos^{1.2} \theta} \right]^{\frac{1}{2}} - 0.020\Sigma \quad (2)$$

$$D' \simeq \frac{D}{\cos \theta} \quad (3)$$

The constant factors and cosine powers were derived from simulation fits and by optimization on Crab Nebula data (taken at a range of zenith angles) and then compared with simulations for calibration. Data selection criteria $0.125^\circ < L' < 0.3^\circ$, $0.05^\circ < W' < 0.135^\circ$, $0.28^\circ < D' < 2.2^\circ$ are applied to select candidate gamma-ray events (examples of these cuts are shown graphically in Figure 1). Cuts based on these intrinsic parameters were verified to be independent of zenith angle and camera design by application of this method to independent Crab Nebula data taken over the period 1994-2003.

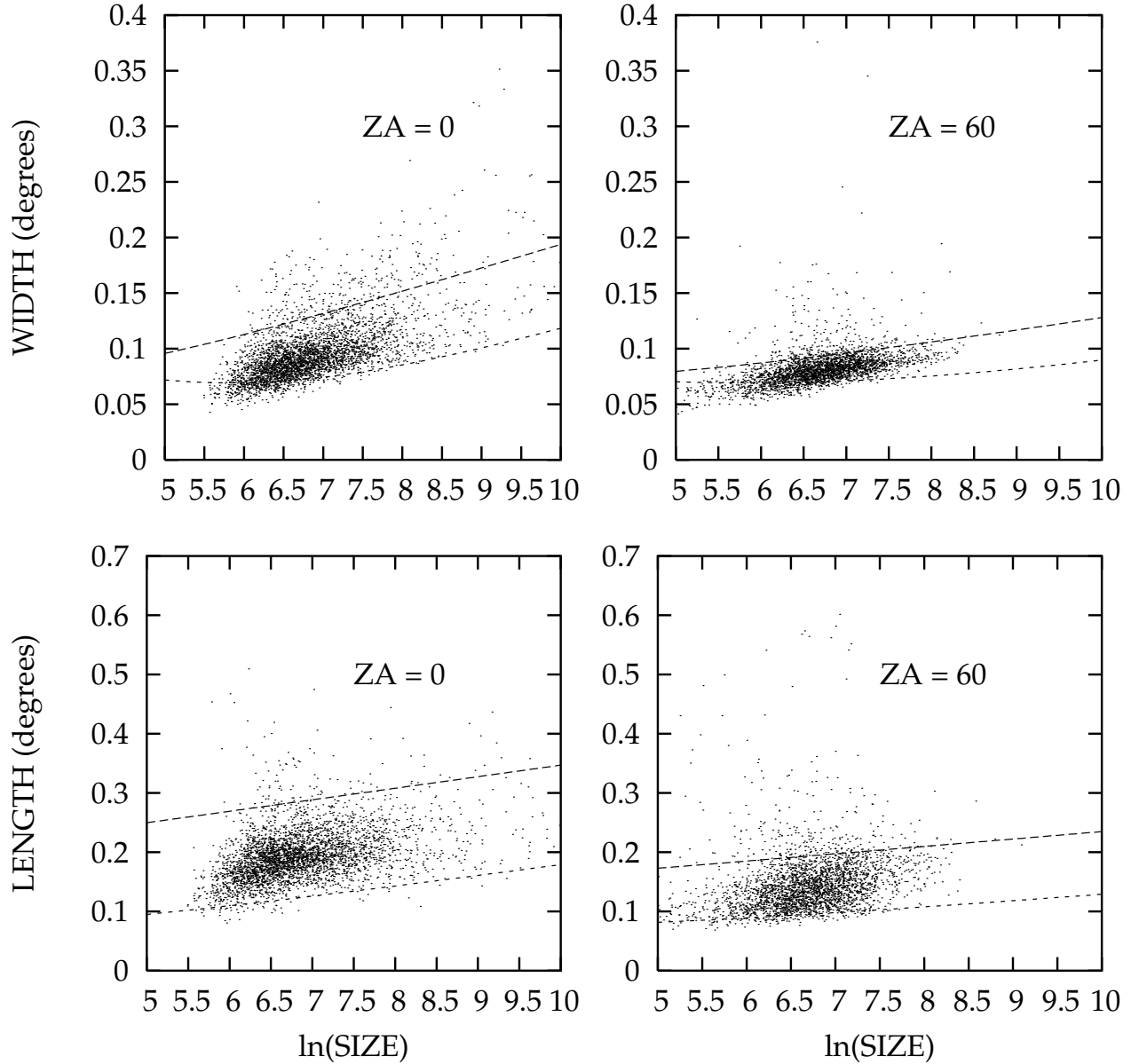


Fig. 1.— Plots of our selection criteria for gamma-ray-like events for two of the parameters (LENGTH and WIDTH) for two different zenith angles (0° and 60°). The dotted lines show the upper and lower cuts on the respective parameters as a function of the SIZE (total signal) parameter. The dots are from simulations of gamma rays with a range of energies.

4. Results

We have combined observations of Sgr A* from 1995 through 2003 resulting in 26 hours of on-source exposure at an average zenith angle of 61° . To determine the pointing offset, observations

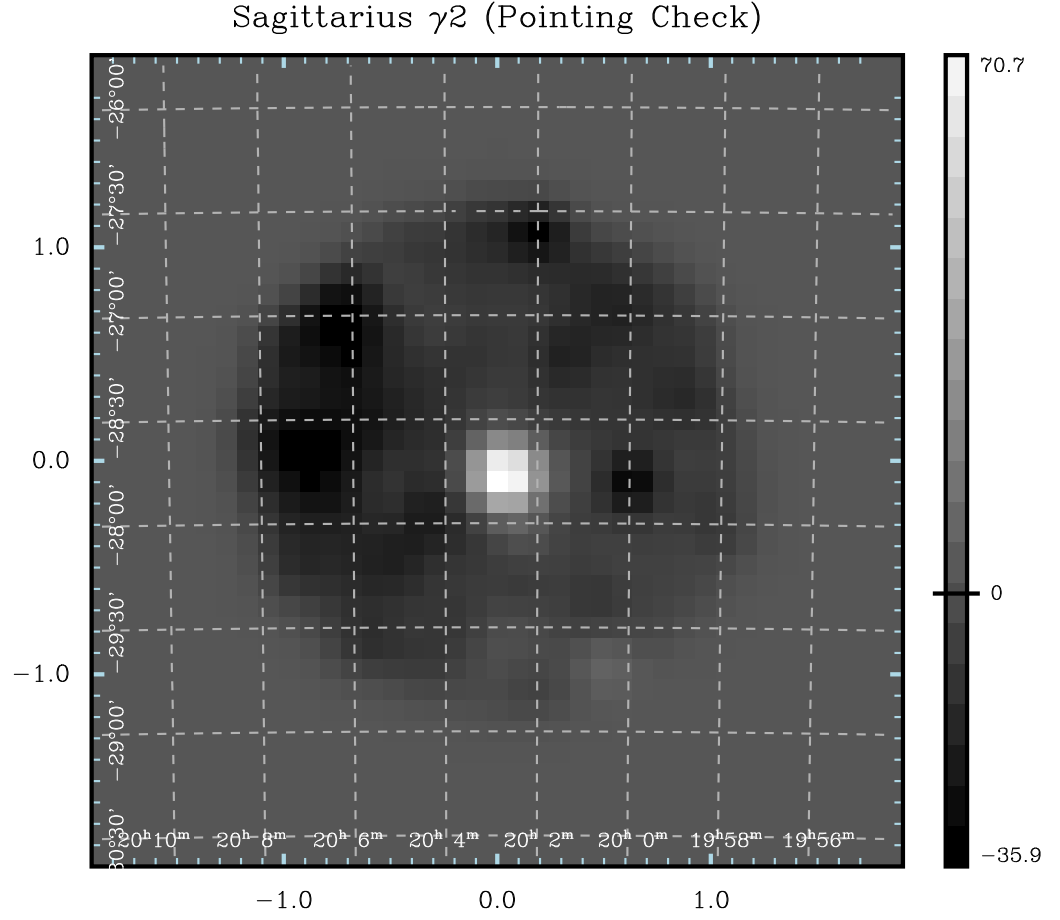


Fig. 2.— Optical image of a star (Sgr γ_2) used to check the telescope’s pointing at low elevation. This image shows that the telescope has an offset of 0.14 degrees down and to the right of camera center position (0,0).

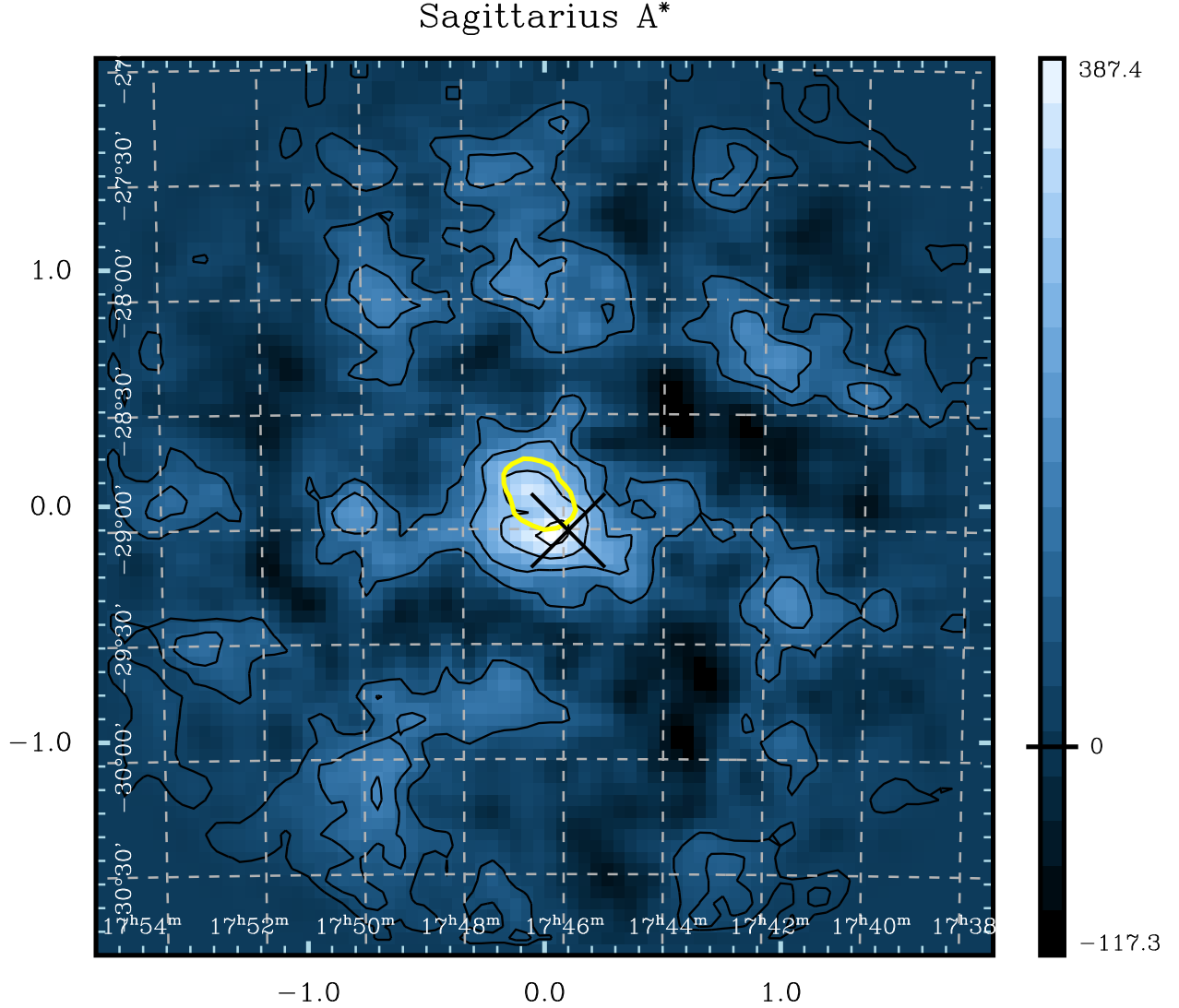


Fig. 3.— A gamma-ray image of the region around Sgr A*. The image is of excess counts with overlaid significance contours (1 standard deviation per contour). The axes are labeled in degrees from the assumed camera center. The true center position of the camera, which is not exactly at (0,0) due to flexing of the telescope at low elevation, is marked with a cross. The dashed lines are the RA and Dec contours at this position. Also shown (as a light contour) is the 99% confidence region for the EGRET observations (Hooper & Dingus 2002).

were taken centered on a nearby bright star (Sgr γ_2) which is at the same elevation as Sgr A*. Using the sky brightness map technique outlined earlier, we determined that the telescope had a pointing offset of 0.14° , as shown in Figure 2. Figure 3 shows the resulting 2-D map of gamma-ray excess with overlaid significance contours. The true center of the camera, correcting for the offset, is plotted as a cross in the image. This image shows a 4.2 standard deviation (σ) excess at the

LZA Crab Nebula

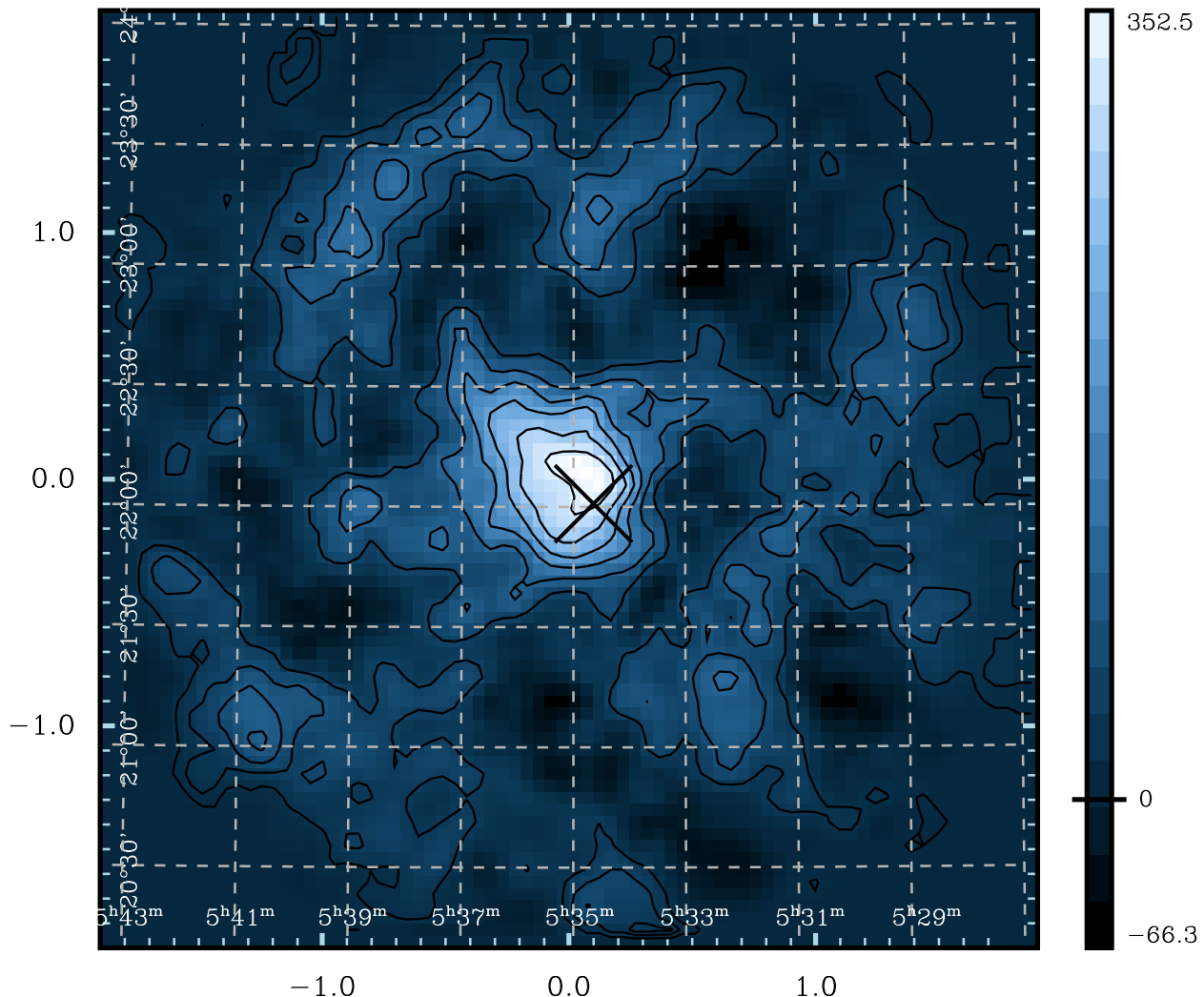


Fig. 4.— A gamma-ray image of the Crab Nebula taken at large zenith angle ($\approx 62^\circ$) using the same analysis procedure used for Sgr A*. The offset and pointing variations can be seen in the resulting image.

corrected center position. To check the robustness of this result, we re-ran the analysis ten times to account for variations due to the Gaussian padding. We find the average significance at the corrected center position is $(3.7 \pm 0.13) \sigma$, somewhat below the initial result. For reference, in Figure 4 we show the results of the same analysis procedure applied to 10 hours of observations of the Crab Nebula at a similar zenith angle range. Note that the significance of 6.1σ of the Crab detection at the offset position is substantially higher than the result of 3.8σ obtained applying the standard small zenith angle analysis procedure to these LZA data. Also, the similar angular extent in the two results indicates consistency with a point source within a 99% confidence region of radius

≈ 15 arcmin. A more detailed analysis of the angular extent would require a prior hypothesis about the nature of the source.

To determine the peak energy of the detected flux from Sgr A*, we simulated gamma rays with a Crab Nebula spectrum (with integral spectral index $\gamma = 1.58$) (Mohanty et al. 1998; Aharonian et al. 2000) and a zenith angle of 61° , and analyzed the resulting data with a detector simulation and our analysis software. We determined the peak detected energy to be ≈ 2.8 TeV. Noise padding and a higher trigger threshold makes this result slightly higher than has been previously reported (Krennrich et al. 1999), and we estimate a 20% systematic error in this energy threshold. We then analyzed a set of real LZA Crab Nebula data runs to find the Crab count rate and compared this to the corresponding rate for Sgr A*. The integral flux for Sgr A*, normalized to the Crab, is then:

$$F_{SgrA}(> 2.8 \text{ TeV}) = N_{0,Crab} \cdot \frac{(2.8 \text{ TeV})^{-\gamma}}{\gamma} \cdot \frac{R_{SgrA*}}{R_{Crab}} \quad (4)$$

Where $N_{0,Crab}$ is the flux normalization factor for the Crab Nebula ($3.12 \times 10^{-7} \text{ m}^{-2} \text{ s}^{-1}$), γ is the integral Crab spectral index, and R_{SgrA*} and R_{Crab} are the corresponding Sgr A* and Crab Nebula gamma-ray count rates. From the LZA Crab data, we find a gamma-ray rate of $R_{Crab}(> 2.8 \text{ TeV}) = 0.501 \pm 0.087 \text{ photons min}^{-1}$ and from Sgr A* we obtain an average rate of $R_{SgrA*}(> 2.8 \text{ TeV}) = 0.205 \pm 0.057 \text{ photons min}^{-1}$. Hence, the gamma-ray flux from the Galactic Center region above 2.8 TeV is $1.6 \times 10^{-8} \pm 0.5 \times 10^{-8}(\text{stat}) \pm 0.3 \times 10^{-8}(\text{sys}) \text{ photons m}^{-2} \text{ s}^{-1}$, or about 0.4 times that of the Crab Nebula (the flux error includes the uncertainty in the Crab Nebula measurement).

The count rate from Sgr A* is shown as a function of time in Figure 5. To determine the probability for steady emission, a χ^2 fit of a constant function ($f(t) = A$) was applied to this data and, for comparison, to a series of data taken of Mrk 421 (a source which is known to be highly variable) at a similar zenith angle range as Sgr A*. The total significance of this Mrk421 data sample was 2.3σ . The Sgr A* data yields a constant count rate of $6.12 \pm 1.59 \text{ } \gamma \cdot \text{min}^{-1}$ with a reduced χ^2 of 1.13 (with 54 degrees of freedom), which corresponds to a 25% probability that there is no variability. The result for Mrk 421 yields a constant count rate of $6.86 \pm 6.13 \text{ } \gamma \cdot \text{min}^{-1}$ with a reduced χ^2 of 3.03 (with 6 degrees of freedom) and a 1.2% chance of no variability.

5. Discussion

The TeV excess observed near the position of the Galactic Center is unlikely to have occurred by chance and constitutes a probable, as yet unconfirmed, detection of a new TeV source. Possible systematics that could contribute to a false detection include the effects of additional noise from the relatively bright off-source region. While we have largely corrected for these effects, some systematic uncertainties remain. We have taken into account trials factors by formulating an explicit *a priori* hypothesis that we would only look for emission at the exact position of the Galactic Center after a pointing correction was applied. Statistical variations in the analysis method (due to the addition of simulated noise in padding) have been taken into account by repeating the analysis ten times, and

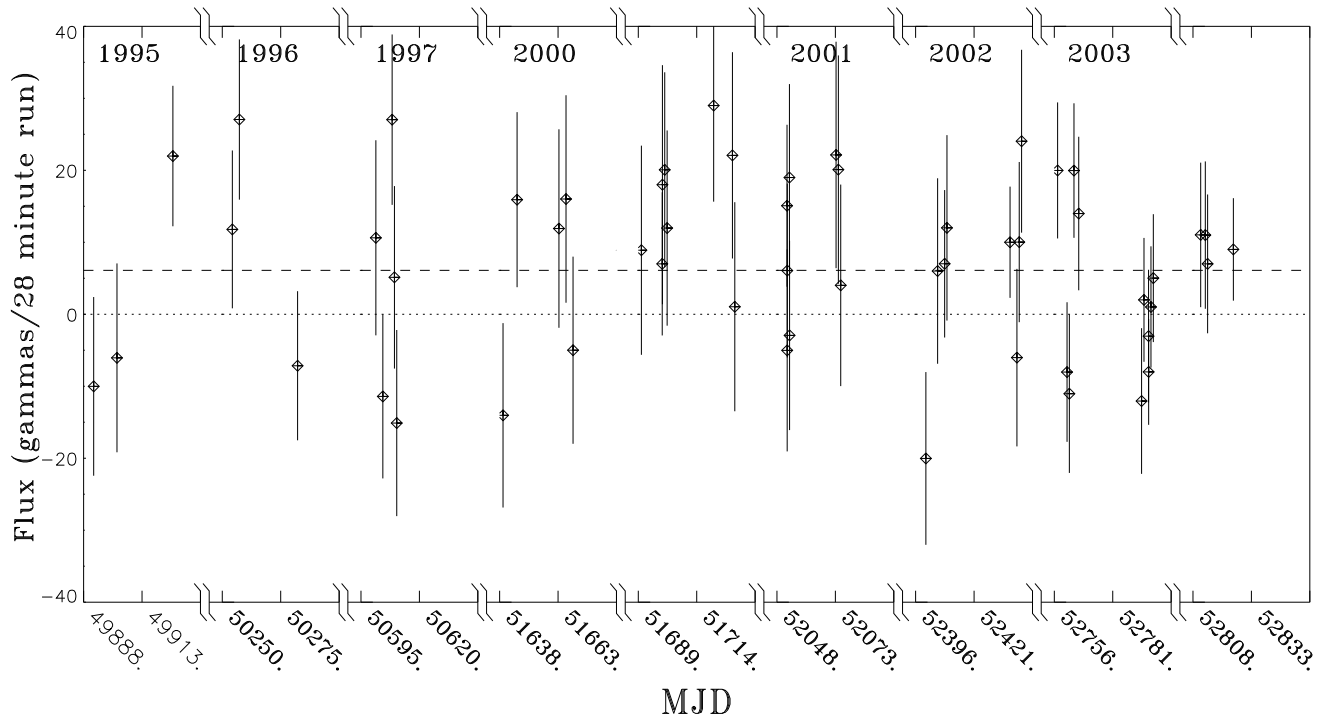


Fig. 5.— Flux of Sgr A* as a function of time. Each data point represents a single 28 minute run. Time gaps in the data have been removed where indicated. The dashed line is a least squares fit of a constant function to the data.

taking the average significance, giving a conservative estimate of 3.7σ for the detection significance.

The lack of significant variability in our data makes it difficult to uniquely identify the source with a compact point source such as Sgr A*, but inspires some confidence in the stability of our observations at large zenith angle. Note that the analysis procedure was designed to mitigate against changes in the count rate due to variations in the instrument. The same ISU simulation package was used here to analyze Whipple observations of the Crab Nebula giving a spectrum in good agreement which that measured a small zenith angle (Krennrich et al. 1999). In the past, our group reported a positive excess of 2.4σ for 1995-1997 observations (Buckley et. al. 1997) and 2.4σ for 1999-2003 observations (Kosack et. al. 2003) at the position of Sgr A*. The combined significance for our refined results is consistent with these earlier analyses. The large error circles for both EGRET (7.2 arcmin) and Whipple (15 arcmin) observations make identification with a particular source difficult, but given the dearth of TeV sources, an accidental angular coincidence of a new source along the line of sight is unlikely, and it is probable that the emission comes from a non-thermal source physically near the Galactic Center.

The high level of emission ≈ 0.4 Crab at a distance of roughly four times that of the Crab Nebula, qualifies this as an unusually luminous galactic source. Previous TeV observations of

relatively nearby galactic sources such as X-ray binaries and shell-type and plerionic supernovae have produced numerous upper-limits, or (at best) unconfirmed detections, making the detection of such an object at 8.5kpc even more unlikely. Mayer-Hasselwander et al. (1998) came to a similar conclusion about the GeV emission based on the high luminosity of the EGRET unidentified source and lack of significant variability. If the Sgr A East supernova shock were the source of the EGRET gamma rays, it would have been an unusually intense explosion (Khokhlov & Melia 1996) and a density of 1000 cm^{-3} and magnetic field of $B \sim 0.18 \text{ mG}$ (well above the canonical values) would be required (Fatuzzo & Melia 2003). While a typical galactic source such as an SNR, pulsar, or stellar mass black hole is unlikely, an active nucleus at our Galactic Center is still a viable possibility and the detection of correlated variability in future gamma-ray and X-ray observations is required to make the identification with Sgr A* compelling. If we associate this emission with either the super-massive black hole Sgr A* or supernova remnant Sgr A East, the observed emission could come from self-Compton scattering by electrons with energies up to at least 2.8 TeV or from pion-decay gamma-rays from primary protons of even higher energy (kinematics require their energy to be at least several times the maximum gamma-ray energy).

The lack of significant variability and the consistency with the Galactic Center position allow more exotic possibilities such as the annihilation of very high mass ($> 2 \text{ TeV}$) dark matter particles at the Galactic Center. While not particularly constraining, these results and a more detailed analysis of the spectrum will be used to derive upper limits for dark matter annihilation in a subsequent paper.

In summary, based on 26 hours of data taken with the Whipple 10m gamma-ray observatory, we report a probable detection of a gamma-ray point source consistent with the position of the Galactic Center. We also describe a modified analysis procedure that we have developed to analyze gamma-ray data taken by Imaging Atmospheric Čerenkov telescopes operating at large zenith angles. The continued observation of TeV gamma rays from the Galactic Center has important theoretical implications for understanding a variety of astrophysical phenomena in the nuclear region of the Milky Way.

Acknowledgements We would like to thank Fluvio Melia, Paolo Gondolo, Johnathan Katz, and Ramanath Cowsik for useful discussion. The VERITAS Collaboration is supported by the U.S. Dept. of Energy, N.S.F., the Smithsonian Institution, P.P.A.R.C. (U.K.) and Enterprise-Ireland.

REFERENCES

- Aharonian, F. A., et al. 2000, *ApJ*, 539, 317
 Baganoff, F. K. et al. 2001, *Nature*, 413, 45
 Baganoff, F. K. et al. 2003, *ApJ*, 591, 891

- Balick, B. and Brown, R. L. 1974, *ApJ*, 194, 265
- Bélanger, G. et al. 2004, *ApJ*, 601, L163
- Bergstrom, L. 1989, *Particle Astrophysics: Forefront Experimental Issues*, 255
- Bergström, L., Ullio, P., & Buckley, J. H. 1998, *Astroparticle Physics*, 9, 137
- Buckley, J. H. et al. 1997, *Proceedings of 25th ICRC (Durban)* 3, 237.
- Dubinski, J. & Carlberg, R. G. 1991, *ApJ*, 378, 496
- Fatuzzo, M. & Melia, F. 2003, *ApJ*
- Ghez, A. M. et al. 2002, *Bulletin of the American Astronomical Society*, 34, 1219
- Ghez, A. M. et al. 2004, *ApJ*, 601, L159
- Giudice, G. F. & Griest, K. 1989, *Phys. Rev. D*, 40, 2549
- Gondolo, P. & Silk, J. 1999, *Physical Review Letters*, 83, 1719
- Hartman, R. C. et al. 1999, *ApJS*, 123, 79
- Hillas, A.M. 1995, *Proceedings of 19th ICRC (La Jolla)*, vol 3
- Hooper, D. and B. Dingus, 2002, *ArXiv Astrophysics e-prints*, astro-ph/0212509.
- Hunter, S. D. et al. 1997, *ApJ*, 481, 205
- Jungman, G. & Kamionkowski, M. 1995, *Phys. Rev. D*, 51, 3121
- Khokhlov, A. & Melia, F. 1996, *ApJ*, 457, L61
- Kosack, K. et al. 2001, *Proceedings of 27th ICRC (Hamburg)*.
- Kosack, K. et al. 2003, *Proceedings of 28th ICRC (Tsukuba)*.
- Krennrich, F. et al. 1999, *ApJ*, 511, 149
- Lessard, R. W., Buckley, J. H., Connaughton, V., & Le Bohec, S. 2001, *Astroparticle Physics*, 15, 1
- Liu, S. & Melia, F. 2002, *ApJ*, 566, L77
- Mayer-Hasselwander, H. A. et al. 1998, *A&A*, 335, 161
- Merritt, D. 2003, *ArXiv Astrophysics e-prints*, astro-ph/0311594
- Mohanty, G., et al. 1998, *Astroparticle Physics*, 9, 15
- Navarro, J. F., Frenk, C. S., & White, S. D. M. 1996, *ApJ*, 462, 563

- Reynolds, P. T. et al. 1993, ApJ, 404, 206
- Rudaz, S. 1989, Phys. Rev. D, 39, 3549
- Schödel, R. et al. 2002, Nature, 419, 694
- Silk, J. & Bloemen, H. 1987, ApJ, 313, L47
- Stecker, F. W. & Tylka, A. J. 1989, ApJ, 343, 169
- Tanimori, T. et al. 1994, ApJ, 429, L61
- Tsuchiya, K. et al. 2003. Proceedings 28th ICRC (Tsukuba).
- Yuan, F., Markoff, S., & Falcke, H. 2002, A&A, 383, 854
- Yuan, F., Quataert, E., & Narayan, R. 2003, ArXiv Astrophysics e-prints, astro-ph/0304125